ACS APPLIED MATERIALS & INTERFACES

Research Article

www.acsami.org

# Bicompartmental Phase Transfer Vehicles Based on Colloidal Dimers

Sijia Wang and Ning Wu*

Department of Chemical & Biological Engineering, Colorado School of Mines, 1500 Illinois Street, Golden, Colorado 80401, United States

Supporting Information

**ABSTRACT:** Colloidal particles have been used extensively for stabilizing oil−water interfaces in petroleum, food, and cosmetics industries. They have also demonstrated promising potential in the encapsulation and delivery of drugs. Our work is motivated by challenging applications that require protecting and transporting active agents across the water−oil interfaces, such as delivering catalysts to underground oil phase through water flooding for in situ cracking of crude oil. In this Research Article, we successfully design, synthesize, and test a unique type of bicompartmental targeting vehicle that encapsulates catalytic molecules, finds and accumulates at oil−water interface, releases the catalysts toward the oil phase, and performs hydrogenation reaction of unsaturated oil. This vehicle is based on colloidal dimers that possess structural anisotropy between two compartments. We encapsulate active species, such as fluorescent dye and catalytic molecules in one lobe which consists of un-cross-linked polymers, while the other polymeric lobe is highly cross-linked. Although dimers are dispersible in water initially, the un-cross-linked lobe swells significantly upon contact with a trace amount of oil in aqueous phase. The dimers then become amphiphilic, migrate toward, and accumulate at the oil−water interface. As the un-cross-linked lobe swells and eventually dissolves in oil, the encapsulated catalysts are fully released. We also show that hydrogenation of unsaturated oil can be performed subsequently with high conversion efficiency. By further creating the interfacial anisotropy on the dimers, we can reduce the catalyst release time from hundred hours to 30 min. Our work demonstrates a new concept in making colloidal emulsifiers and phase-transfer vehicles that are important for encapsulation and sequential release of small molecules across two different phases.

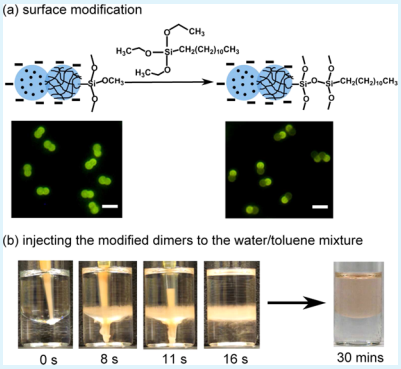


**KEYWORDS:** *compartment, colloid, phase transfer, dimer, emulsifier*

## INTRODUCTION

Colloidal particles that are partially wettable to both oil and water tend to adsorb at an oil−water interface. Once adsorbed, they are very stable because of the high energy barrier of desorption,[1] which offers a great advantage over molecular surfactants. As such, micro- and nanoparticles have long been used in the petroleum, cosmetic, food, and pharmaceutical industries[2−11] to stabilize emulsions and foams against coalescence. However, the stabilization energy of a particle with homogeneous surface properties depends sensitively on its contact angle at the interface,[12] which is often difficult to tune precisely.

Better control of the particle wettability can be achieved if its surface can be tailored differently on two sides of the particle, that is, the so-called Janus particle.[13−17] For example, when one side is coated with hydrophilic molecules and the other side is hydrophobic, the Janus particle can mimic the amphiphilic nature of molecular surfactants faithfully. Recent work using Janus spheres as colloidal emulsifiers[18−20] have shown significant advantages over isotropic particles. The spherical geometry, however, is still far from ideal. It is widely known that the geometric balance between the hydrophilic and lipophilic parts of molecular surfactants largely dictates different morphologies that they can pack into and influences their emulsification behavior.[21] Motivated by this, very recently, Park and Lee[22,23] performed theoretical calculations on the attachment energy of colloidal dimers, whose interfacial and geometric asymmetry can be, in principle, tailored independently. They have found that amphiphilic dimers can adopt upright or tilted orientations at the oil−water interface, depending on the relative difference in both diameter and hydrophilicity between two lobes. Recent experiments appear to support the theoretical findings.[24,25]

Although most studies focused primarily on the adsorption of particles at oil−water interfaces, in many applications it is also important to transfer species such as molecules and nanoparticles across the interface.[26−29] For example, drug-carrying vehicles that can enter various types of biological barriers from plasma can revolutionize modern diagnostic and therapeutic technologies. Our research here is motivated by a similar problem facing the petroleum industry in extracting unconventional hydrocarbons such as heavy oil.[30] In spite of its immense resource, only 15% percent of yearly oil production is from heavy oil due to its notoriously high viscosity. Conventional water flooding fails because less viscous water can easily find pathways to flow through a reservoir (i.e., the fingering effect)

Received: August 25, 2014
Accepted: October 16, 2014
Published: October 16, 2014

  

and leave pockets of oil behind. Even if heavy oil is extracted to the surface, its viscosity must be kept low for transportation in pipelines. Therefore, the Society of Petroleum Engineers[30,31] has recently identified that downhole delivery of nanocatalysts for in situ conversion of heavy oil into a lighter grade could be a game-changing technology. The central task for realizing in situ cracking is the delivery of catalytic species into the oil phase through downhole porous media. This process has two competing constraints: the catalysts must first be dispersed in water and then delivered underground through water flooding; later they need to accumulate in the oil phase for subsequent catalytic reactions such as low-temperature oxidation or partial hydrogenation. It is particularly challenging for catalysts since they usually are not amphiphilic in nature. Surface functionalization could be detrimental to their catalytic activities.[32]

Here, we design, synthesize, and test a unique type of bicompartmental targeting vehicle that can fulfill this challenging task for oil-phase delivery of catalysts. As shown in Figure 1, the targeting vehicle is designed based on a two-compartmental polystyrene particle where one non-cross-linked compartment encapsulates the catalysts. The other compartment consists of highly cross-linked polymer. Although the vehicle is hydrophilic and dispersible in water initially, it can become amphiphilic because the non-cross-linked compartment swells in oil easily. This will enable the vehicle to transport through the aqueous phase; seek and then attach to the oil–water interface. Furthermore, the non-cross-linked compartment is designed to swell significantly and dissolve in oil eventually, which will facilitate the targeted release of catalysts into the oil phase.

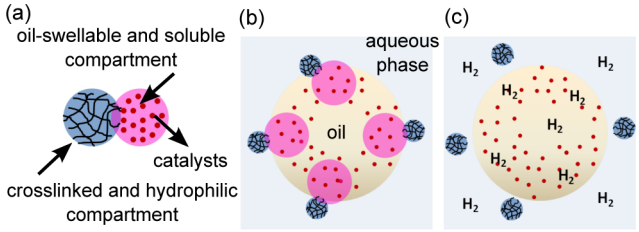


**Figure 1.** Schematic of the bicompartmental vehicle (colloidal dimer) targeted for delivering catalysts to oil phase underground. (a) One compartment is hydrophilic and highly cross-linked, while the other one is non-cross-linked and oil-swellable. (b) The vehicle transports through water flooding, adsorbs at the oil–water interface, and swells significantly in oil. (c) The hydrophobic compartment eventually dissolves in oil and releases catalysts for subsequent hydrogenation.

## EXPERIMENTAL METHODS

**Chemicals.** Styrene, divinylbenzene (DVB), sodium 4-vinylbenzenesulfonate, polyvinylpyrrolidone (PVP, $M_w$ = ~40 000), sodium dodecyl sulfate (SDS), 3-aminopropyltriethoxysilane, Oil Red O, chlorotris(triphenylphosphine)rhodium(I)) (the Wilkinson's catalyst), palladium(II) acetate ($Pd(OAc)_2$), and n-dodecyltriethoxysilane are purchased from Sigma-Aldrich. 3-(Trimethoxysily) propyl acrylate (TMSPA) is purchased from Tokyo Chemical Industry (TCI). The thermal initiator V65 is bought from Wako Chemicals. All chemicals are used as received except that both styrene and divinylbenzene are purified by aluminum oxide before usage.

**Synthesis of Polystyrene Dimers.** The synthetic route we use to make colloidal dimers is based on seeded emulsion polymerization.[33] We prepare the seed polystyrene (PS) spheres by dispersion polymerization.[34] After we clean the PS seeds four times via centrifugation at 4000 rpm (30 min), we can further use these seeds for making cross-linked PS spheres. In brief, we use a tip sonicator (Branson digital sonifier 450) to make an aqueous emulsion. The aqueous phase consists of 4 mL of 5 wt % PVP and 0.5 mL of 2 wt % SDS. The oil phase is made up of 1 mL of styrene, 0.05 mL of DVB, 0.05 mL of 3-trimethoxysily propyl acrylate, and 0.02 g of V65. We mix the emulsion with 1 mL PS seeds (10 wt %) for 24 h, then put the swollen seeds in an oil bath (70 °C) for another 24 h for polymerization. We then clean these cross-linked PS via centrifugation for four times again. By further swelling the cross-linked PS with an emulsion of styrene, PS dimers can be formed. We can tune the size of the newly formed lobe (i.e., the second lobe) by adjusting the amount of styrene to swell the cross-linked PS seeds. Finally, we perform polymerization at 70 °C overnight to solidify the second (non-cross-linked) lobe.

**Dye/Catalyst Encapsulation.** To encapsulate Oil Red O, palladium(II) acetate, or the Wilkinson catalysts in the non-cross-linked lobe, we mix 0.5 mL of styrene, 2 wt % V65, and variable amounts (from 5 to 100 mg/mL) of the above molecules. They are emulsified in an aqueous solution of 4 mL of 5 wt % PVP and 0.5 mL of 2 wt % SDS. The emulsion is then used to swell 1 mL cross-linked PS seeds (1 wt %) for ~24 h. Subsequently, polymerization is performed at 70 °C for another 24 h. The synthesized dimers are then cleaned four times via centrifugation.

**Surface Modification.** The incorporation of vinylsilane molecules (e.g., TMSPA) in the cross-linked lobe allows us to modify its surface properties after the dimer encapsulation and synthesis. For example, we add 1 mL of 0.1 wt % dimers and 100 μL of *n*-dodecyltriethoxysilane into an ethanol/water mixture (95:5 vol %), with stirring for 24 h at room temperature. We then wash the particles by methanol four times via centrifugation (2000 rpm for 20 min).

**Rhodamine 6G coating on polystyrene dimers.** We mix 1 mL of dimer (0.5 wt %) with 12.5 μL of rhodamine 6G solution (0.25 wt %) overnight. Then we centrifuge the particles four times before taking fluorescent images.

**Biphasic Delivery.** We put equal amount (1–2 mL) of toluene and water in a glass vial. Dimers with different encapsulated molecules are then injected to the water phase. Typically, the vial is sit on the bench without disturbance during the delivery. Occasionally, we put the vial on a rotator with constant rotation of 50 rpm to accelerate the delivery time.

**Hydrogenation of Olefin.** We mix 40 μL of octene, styrene, or butyl acrylate with 2 mL of toluene, as the oil phase. After the catalyst molecules are released from the dimers, we collect 1 mL of the upper oil phase, dilute it 10 times with toluene, and carry out the hydrogenation reactions in a closed chamber, where hydrogen gas is injected at 2 bar. The hydrogenation takes place at 80 °C for 1 h.

**Characterization.** The morphologies of conventional dimers are characterized by scanning electron microscopy (JEOL JSM-7000F). To ensure dye encapsulation, dimers are also imaged by fluorescent microscopy. We also use nuclear magnetic resonance (JEOL ECA-500) to detect the existence of dissolved polystyrene chains in oil phase. The encapsulation efficiency of the Wilkinson's catalysts in the dimers is determined by the following procedures. Since the equipment (ICP-OES PerkinElmer Optima 5300 DV) we use is only capable of quantifying the metal ion concentration in aqueous solution, we need to dissolve the metal salts in water. After all the catalysts in the dimers are delivered to the oil phase, we take 10 μL of liquid from the oil phase and dilute it with 990 μL of toluene. We then evaporate all toluene in 1 mL of the above solution (with 100 times dilution of the original oil phase) at 50 °C. Subsequently we add 5 mL of water and 2 mL of 30% hydrogen peroxide in the vial and heat for 1 h (100 °C). This process can be repeated for multiple times until a clear solution is obtained, when the organic compounds in the catalytic molecules are fully decomposed. We then add 10 mL of 2% $HNO_3$ to dissolve the metal ions in aqueous solution. Afterward, we use inductively coupled plasma optical emission spectroscopy (ICP-OES PerkinElmer Optima 5300 DV) to measure the metal concentration in the solution. Finally, we calculate the catalyst encapsulation efficiency based on the amount of metal salts delivered to the oil phase and the amount of particles we injected in the vial. In the calculation, we

assume that all catalysts in the dimers are released to the oil phase. To quantify the degree of conversion of olefins, we use a gas chromatography–mass spectrometry (GC-MS Varian 1200L) with triple quad analyzer to analyze the compositions of the oil phase after the hydrogenation experiments.

## RESULTS AND DISCUSSION

**Dimer Synthesis and Active-Agent Encapsulation.** Figure 2 summarizes the synthetic routes we follow to make

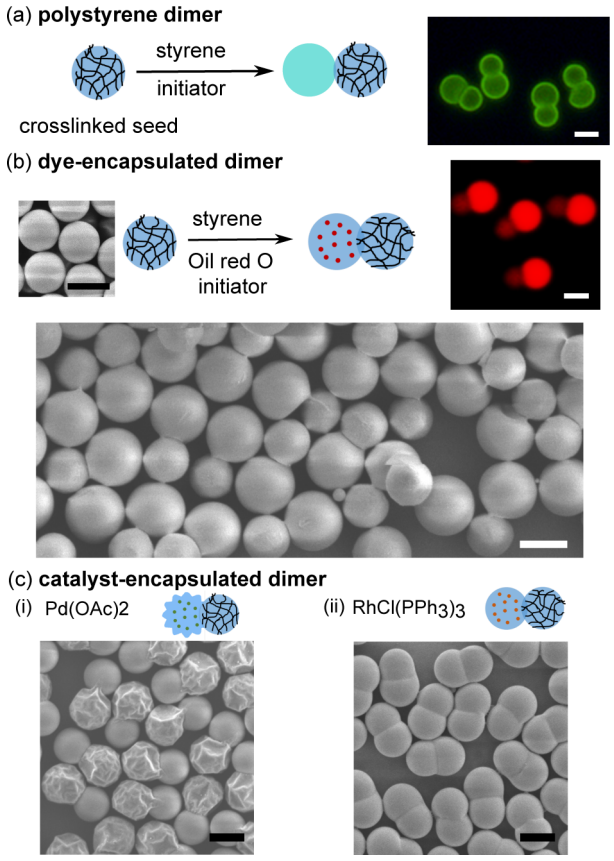


**Figure 2.** Synthetic route of polystyrene dimers encapsulating different molecules. (a) Synthesis of conventional polystyrene dimers. Fluorescent image shows that the negatively charged dimers absorb positively charged fluorophores (i.e., rhodamine 6G) uniformly. (b) The fluorescent image shows selective encapsulation of Oil red O in the un-cross-linked lobe. The SEM image shows the large-field view of polymerized dimers. (c) Encapsulation of two molecular catalysts in the un-cross-linked lobe. Scale bar for all images: 2 $\mu$m.

both conventional polystyrene dimers and those encapsulated with different kinds of active agents. The conventional dimers are synthesized based on a seeded emulsion polymerization method.[33,35−39] We first swell polystyrene spheres with styrene, divinylbenzene, and a small amount of vinylsilane (e.g., 3-(trimethoxysily) propyl acrylate) to make cross-linked polystyrene spheres, that is, the seeds. In the second stage, styrene is used again to swell the seeds. As shown in Figure 2a, the elastic energy of the cross-linked polymer prevents itself from isotropic swelling, induces a phase separation between the monomer and the seeds, and gives rise to the second (monomer) lobe. Further polymerization will solidify the second lobe and generate dimers with high monodispersity. To prevent dimer aggregation in water, we add a small amount of ionic monomer (e.g., sodium 4-vinylbenzenesulfonate) when synthesizing the seed PS spheres. Interestingly, when we swell the cross-linked seeds with styrene again, some poly(sodium 4-styrenesulfonate) chains migrate toward the second lobe. Later we will exploit this property for oil-phase delivery of catalytic molecules. This is evidenced by the fluorescent image in Figure 2a, where the positively charged fluorophores (Rhodamine 6G) are absorbed uniformly on both lobes. The surface charges arising from sulfonate functional groups stabilize polystyrene dimers in water. Although the dimer has very similar surface and bulk compositions in both lobes, their physical properties are inherently different. One lobe is made of highly cross-linked (e.g., 5%−20%) polymer while the other lobe primarily consists of linear chains.

As shown in Figure 2b and 2c, the synthetic recipe for conventional dimers can be conveniently modified to encapsulate different kinds of oil-soluble molecules in the second and non-cross-linked lobe. As a proof of principle, we mix styrene with a fluorescent molecule Oil Red O (ORO), which is then used to swell the cross-linked seed particles. The fluorescent image in Figure 2b clearly demonstrates the selective encapsulation of ORO in the second lobe. The large-field SEM image in Figure 2b also shows that the encapsulation does not interfere with the dimer synthesis in general and the particle monodispersity can be preserved. We further apply the similar synthetic strategy to encapsulate two other types of molecular catalysts $Pd(OAc)_2$ and $RhCl(PPh_3)_3$. Both of them are common catalysts for hydrogenation of alkenes. When $Pd(OAc)_2$ is loaded close to its solubility limit in styrene (~5 mg/mL), the second lobe undergoes significant buckling (Figure 2c-i) during the polymerization stage. This is probably caused by the poor compatibility between polystyrene and $Pd(OAc)_2$.[40] The morphologies of dimers that encapsulate $RhCl(PPh_3)_3$), however, are similar to conventional dimers (Figure 2c-ii).

**Structural Emulsifier.** We first study the behavior of the conventional polystyrene dimers (without any encapsulation or surface modification) in a mixture of toluene and water. Since the dimers possess a uniform distribution of sulfonate groups on their surfaces, they are well dispersed in the aqueous phase initially (Figure 3a). They sediment to the bottom of the vial within ~1 day because of their large size (~1.6 $\mu$m for both lobes) and higher density (~1.05 g/cm$^3$) than water. Afterward, they surprisingly migrate to the water–toluene interface. After ~72 h, no particle is left at the bottom and both oil and water phases are clear. Essentially all dimers are trapped at the interface. To understand what happens, we examine the shape of dimer particles using an optical microscope. Figure 3b shows that the dimers are symmetric initially. As time progresses, one of the lobes becomes significantly larger due to swelling by toluene, while the other lobe barely changes its size. Therefore, the autonomous movement of our dimers toward the toluene-water interface can be understood by the physical anisotropy in the dimers. Toluene, although immiscible with water, has a small solubility of 0.52 g/L at 25 °C. This trace amount of toluene in water is sufficient enough to preferentially swell the non-cross-linked lobe because of the much favorable mixing enthalpy between toluene and linear polystyrene chains.[41,42] When sufficient amount of toluene is absorbed in one lobe, the dimer not only becomes amphiphilic but lighter than water. For instance, if the non-cross-linked lobe doubles its size from 1.6 to 3.2 $\mu$m because of swelling, the dimer density will change from 1.05 to 0.91 g/cm$^3$. Buoyancy can drive the particles toward the toluene-water interface. Since the cross-linked lobe

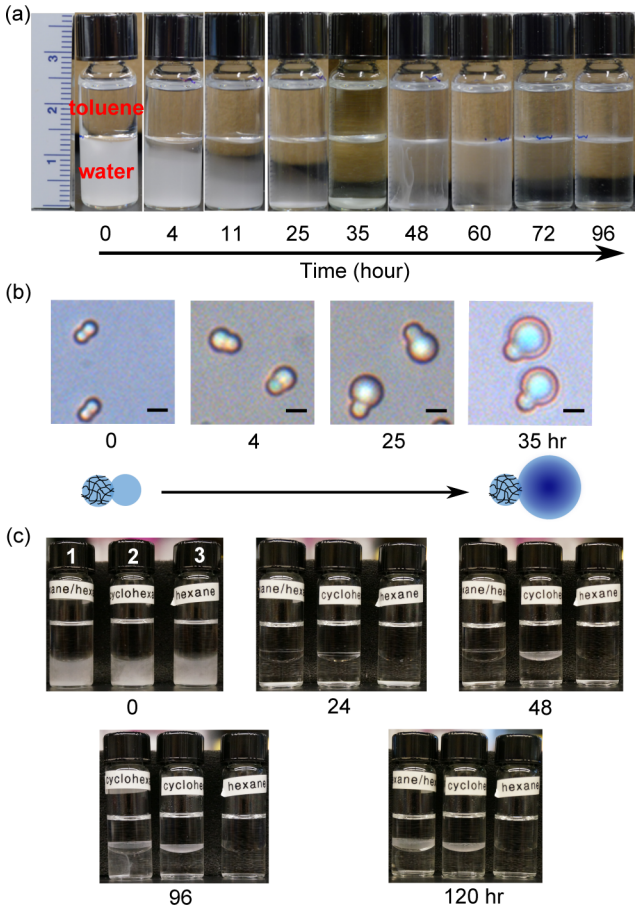


**Figure 3.** (a) Time evolution of the conventional polystyrene dimers in water/toluene biphasic solution. The scales on the ruler are in cm. (b) Optical image of dimers at the interface in different time. The non-cross-linked lobe absorbs oil significantly. Scale bar: 2 $\mu$m. (c) Oil phase composition affects the migration of polystyrene dimers toward the interface. At time zero, the upper phases in three vials are (1) 50%:50% mixture of cyclohexane and hexane, (2) 100% cyclohexane, and (3) 100% hexane, respectively. The bottom phase is water (with dimers) in all vials.

is nonswollen and remains hydrophilic, the dimers stay at the interface.

Our experiment demonstrates that the conventional polystyrene dimers can be used as colloidal emulsifier even without modifying its surface property. We note that it represents a different kind of emulsifier than other kinds of colloidal surfactants, which often need to have a contact angle close to 90°.[15−17,38,43,44] Our dimers are hydrophilic initially and they can be easily dispersed in aqueous phase. They, however, quickly convert into amphiphilic particles by absorbing even a trace amount of oil. In fact, the amphiphilicity becomes quite strong since oil essentially soaks into one of the lobes while the other remains hydrophilic. Because the behavior of our dimers is primarily due to the structural difference (i.e., cross-linked vs non-cross-linked) between two lobes, we coin them structural emulsifiers. Another noticeable difference between our dimers and conventional emulsifiers is the buoyancy effect since the oil-swollen particles can become lighter than water, which helps them find the oil phase under natural conditions in underground reservoirs.

We notice that the structural emulsifier works under two conditions: (1) colloids need to be swollen by oil at least partially; (2) oil must have some solubility in water. When we change the upper oil phase into linear hydrocarbons, such as hexane, our dimers remain settled at the bottom of the vials because of its negligible solubility in water (9.5 mg/L) and poor compatibility with polystyrene (Figure 3c). However, when the oil phase is 100 % cyclohexane or even an equal volume mixture of cyclohexane and hexane, the dimers are able to move toward the water−oil interface. Since crude oil is often a mixture of linear, cyclo, and aromatic hydrocarbons,[45,46] our dimers could find potential applications in enhanced oil recovery. Moreover, the concept presented here can be extended to other oil−water systems if the particle is made of copolymers with both linear and aromatic repeating units, so that it can be swollen by both types of hydrocarbons. Furthermore, unlike conventional colloidal stabilizers whose interfacial properties are homogeneous, the surface properties of two lobes on the dimer particle can be modified independently, which will be discussed later.

**Oil-Phase Delivery and Hydrogenation.** The initially hydrophilic nature of our dimers makes them easily dispersible in water. This is advantageous because those dimers can be transported underground through water flooding, which is commonly used to displace residual oil in reservoir formation. With encapsulated molecular catalysts in the non-cross-linked lobe, our dimer becomes a delivery vehicle that can both find oil and release catalysts to the oil phase for in situ cracking. To demonstrate this concept, we first test the oil-phase delivery of dye molecules. Shown in Figure 4, the dye is initially encapsulated in the non-cross-linked (larger) lobe, rendering the water phase red. The particles gradually move toward the interface when they are swollen by trace amount of toluene in water. Once they are at the interface, the dye molecules diffuse out of the non-cross-linked lobe into the oil phase. One hundred percent phase transfer is complete after ∼1 week when the water phase becomes clear. By examining the particles at the final stage (Figure 4b), we find that the non-cross-linked lobes eventually disappear, indicating that they dissolve completely in the oil phase. The NMR spectra shown in Figure 4c further demonstrate that polystyrene chains (as characterized by the expected resonance for the aromatic proton peaks near 7.1 and 6.6 ppm) can be found in the oil phase but not the water phase. We note that the dissolvability of the non-cross-linked lobe will allow potential encapsulation and release of much larger species such as catalytic nanoparticles in addition to molecular catalysts, which will be tested in future.

We further investigate the oil-phase delivery of organometallic salts which can catalyze the hydrogenation of olefins. Although two salts ($Pd(OAc)_2$ and $RhCl(PPh_3)_3$) have been encapsulated successfully, we primarily focus on the latter (i.e., the Wilkinson's catalyst) because it has higher solubility (10 wt %) in styrene. We inject dimer particles into the aqueous phase in a vial where oil is separated on the top. We then use two different methods to test the oil-phase delivery of catalysts: a static process where the vial sits still on a bench (similar to the dye release experiment, Figure 5a-i) and a dynamic process where the vial is put on a rotator and is subject to a constant rotation speed of 50 rpm (Figure 5a-ii). Clearly, rotation induces a mild degree of mixing, which significantly decreases the amount of time (10 times faster) for complete release of the catalysts. In fact, this release time can be further decreased by at least 2 orders of magnitude when we modify the surface property of the dimers, which will be shown later. The amount

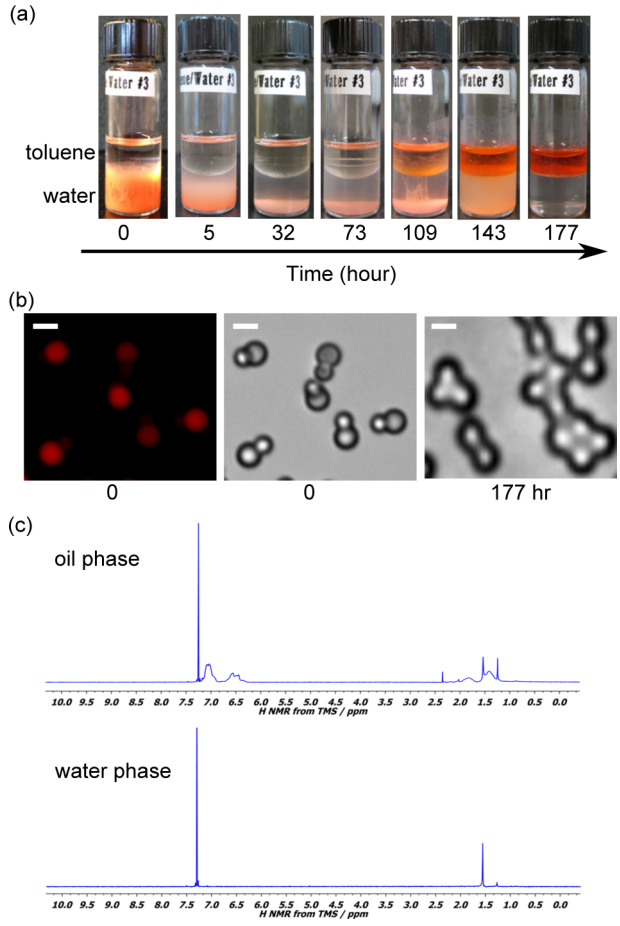


**Figure 4.** (a) Time evolution of the Oil Red O encapsulated dimers in a mixture of toluene and water. (b) When $t$ = 0, both fluorescent and bright-field microscopy images show that the dye is encapsulated in the large and non-cross-linked lobe. At $t \approx 177$ h, the non-cross-linked lobes eventually dissolve in the oil phase. Scale bar for all images: 2 $\mu$m. (c) $^1$H NMR spectra of both oil and water phases. Note that the peak around 7.24 ppm in both images corresponds to the solvent chloroform we use for NMR characterization. The peak near 1.55 ppm corresponds to the residual water.

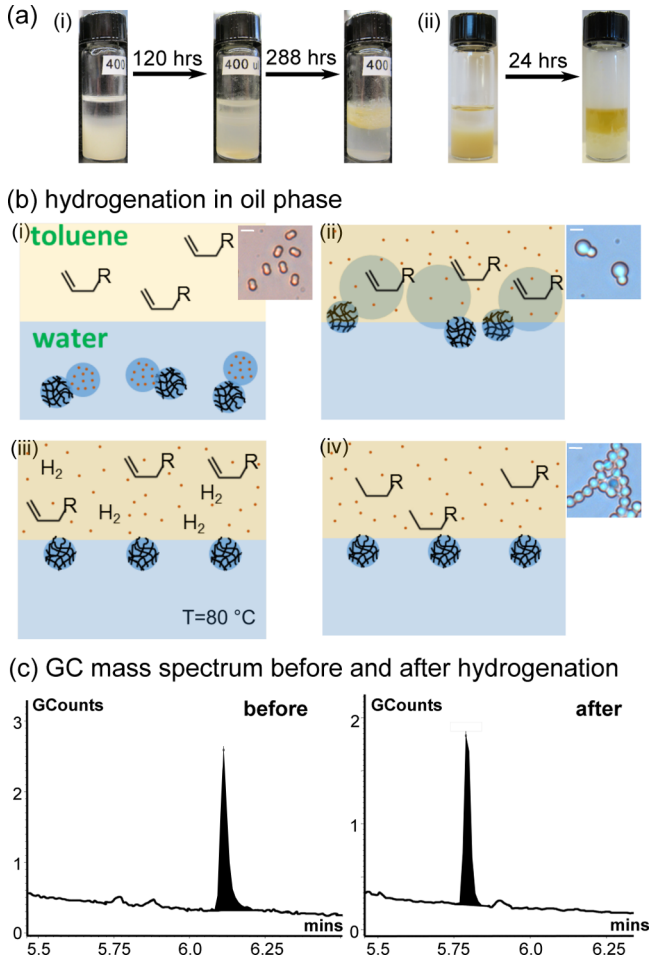


**Figure 5.** Oil-phase delivery of the Wilkinson's catalyst and hydrogenation reaction. (a) $RhCl(PPh_3)_3$ encapsulated in dimers is transported from water (bottom phase) to oil (top phase). The glass vial was (i) put on a bench without disturbance or (ii) put on a rotator with a constant rotation speed of 50 rpm. (b) Schematics illustrate the oil-phase delivery and hydrogenation using dimers. Red dots represent the catalysts. The insets show corresponding microscopy images of the particles. Scale bar: 2 $\mu$m. (c) GC mass spectra of the substrate (styrene) and product (ethylbenzene) before and after the hydrogenation of styrene.

of Wilkinson's catalysts in the oil phase can be determined by the inductively coupled plasma optical emission spectroscopy. For 1 mL of 1 wt % dimers, they deliver ~486 ppm catalysts in 2 mL of toluene. This corresponds to ~12% encapsulation efficiency. Considering that many small polystyrene spheres are formed during the second stage of the dimer synthesis (because of the homogeneous nucleation effect), we believe that catalysts are also encapsulated in these small particles which are then separated from dimers during centrifugation.

After the catalysts are delivered into the oil phase, we perform the hydrogenation reaction for three different kinds of $\alpha$-olefins, that is, styrene as a model for aromatics, octene for linear hydrocarbons, and butyl acrylate for unsaturated esters. Forty microliters of olefins is each dissolved in separated vials of 2 mL of toluene where the Wilkinson catalysts have already been delivered through dimers (see Experimental Methods for details). The mixtures are then heated to 80 °C under 2 bar of hydrogen gas (Figure 5b). After 1 h, we stop the reaction and take the oil phase for GC-mass spectrometry. As shown in Figure 5c, we find that both styrene and octene reach 100% conversion to ethylbenzene and octane, respectively. For butyl acrylate, its conversion to butyl propionate is ~84.5%. Clearly, the high conversion rates prove that our dimer system is capable of performing oil-phase catalytic reactions by delivering the encapsulated catalysts from water to oil.

**Dimer Surface Modification.** We notice that, in our previous experiments, it takes at least several days for dimers to migrate toward the oil–water interface. The time depends on the diffusion of toluene through water phase toward the particles, which have sedimented at the bottom of the vial. The diffusivity of toulene $D$ is ~$9.1 \times 10^{-6}$ cm$^2$/s in water. If the height of water phase $H$ is ~1.5 cm, it will take $t \approx H^2/D \approx 50$ h for toluene to diffuse through, which is consistent with our experimental observation. This time significantly delays the process for complete release of the encapsulated agents. Although we have shown that this process can be sped up by introducing agitation to mix toluene with water (Figure 5a-ii), a more efficient way is to modify the surface properties of the dimers, so that they are amphiphilic on surface property.

The bicompartmental nature of dimers allows us to tune the interfacial hydrophobicity easily. As illustrated in Figure 6a,

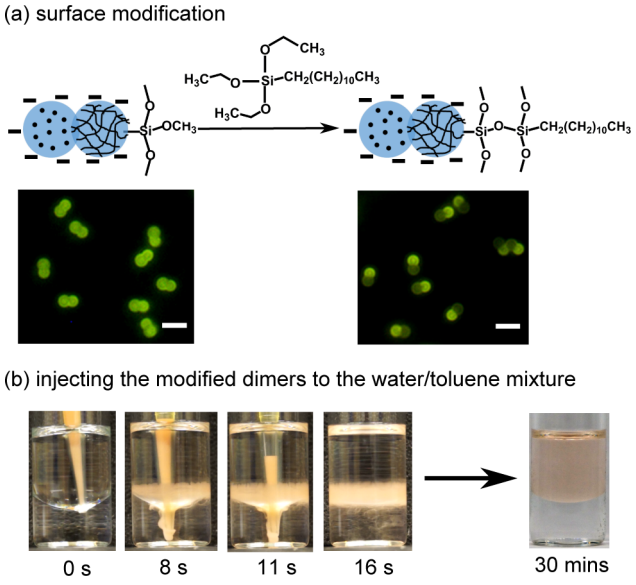


**Figure 6.** (a) Selective attachment of *n*-dodecyltriethoxysilane on the cross-linked lobe renders the dimer amphiphilic. Fluorescent images show the absorption of rhodamine 6G before and after surface modification. Scale bar is the same for both images: 5 $\mu$m. (b) Dye release from the amphiphilic dimers. The first four snapshots show that the amphiphilic dimers accumulate at the interface immediately after injection. All encapsulated dye release to the oil phase within 30 min.

when making the cross-linked seeds, we purposely add a small amount of vinylsilane molecules, that is, the 3-(trimethoxysily) propyl acrylate. This incorporation allows us to modify the surface properties of the cross-linked lobe after the encapsulation of active agents and dimer synthesis. For example, via the conventional sol–gel coupling reaction,[47] we can attach *n*-dodecyltriethoxysilane molecules on the cross-linked lobe so that it becomes more hydrophobic. Since the non-cross-linked lobe remains hydrophilic because of the sulfonate functional groups (Figure 2a), the surface-modified dimers are amphiphilic. We further prove the amphiphilicity by absorbing positively charged fluorophores on dimers before and after the surface modification. As indicated by the images in Figure 6a, the modified dimers show a significant decrease in fluorescence intensity on the cross-linked lobe because of its hydrophobic surface. As Figure 6b and Supporting Information movie 1 show, these amphiphilic dimers go to the oil–water interface immediately even when we inject the particle solution into the water phase. This also significantly reduces the amount of time for agent release, which takes place less than 30 min after the injection.

## CONCLUSIONS

We develop a new type of bicompartment and phase transfer vehicle for molecular catalysts based on colloidal dimers. The polymer in one lobe is cross-linked while the other one is not. Because of this structural anisotropy, we show that dimers can be surface active. Although they are initially dispersible in water, the dimers migrate to the oil–water interface upon contact with a trace amount of oil. This is because the un-cross-linked lobes can be swollen significantly by oil, rendering the dimers amphiphilic. By further encapsulating active species such as fluorescent dye and catalytic molecules in the un-cross-linked lobe selectively, we demonstrate that the dimers can be used as a delivery vehicle to transfer catalysts from water to oil. The successful release of catalysts is further confirmed by hydrogenation of unsaturated oil with high conversion efficiency. Moreover, the phase-transfer time can be significantly reduced when we combine both interfacial and structural anisotropy on the dimer vehicles. The advantages of this new type of colloidal emulsifier and delivery vehicle include: (1) the initial dispersity of particles in water ensures high particle stability and sufficient loading of catalysts or active molecules; (2) the particles do not release materials until they are located at the interface. The active molecules are fully protected until they reach the destination; (3) compared with isotropic particles, the surface properties of our delivery vehicles can be tuned anisotropically on two lobes. Our work demonstrates a new concept in making colloidal emulsifiers and phase-transfer vehicles. The bicompartmental particles developed here could find applications for encapsulation and sequential release of small molecules across two different phases.

## ASSOCIATED CONTENT

### Supporting Information

Movie showing the *n*-dodecyltriethoxysilane modified Oil red O encapsulated dimers go to the toluene–water interface immediately after injection to the water phase. This material is available free of charge via the Internet at http://pubs.acs.org.

## AUTHOR INFORMATION

### Corresponding Author

*E-mail: ningwu@mines.edu.

### Notes

The authors declare no competing financial interest.

## ACKNOWLEDGMENTS

We thank Prof. Ryan M. Richards for his help in the hydrogenation experiments, Prof. James F. Ranville for ICP-OES characterization, and Prof. Edward A. Dempsey for using the GC-mass spectrometry. Acknowledgment is also made to the Donors of the American Chemical Society Petroleum Research Fund (PRF No. 53638-DN110) for support of this research.

## REFERENCES

(1) McGorty, R.; Fung, J.; Kaz, D.; Manoharan, V. N. Colloidal Self-Assembly at an Interface. *Mater. Today* **2010**, *13*, 34–42.

(2) Sullivan, A. P.; Kilpatrick, P. K. The Effects of Inorganic Solid Particles on Water and Crude Oil Emulsion Stability. *Ind. Eng. Chem. Res.* **2002**, *41*, 3389–3404.

(3) Hunter, T. N.; Pugh, R. J.; Franks, G. V.; Jameson, G. J. The Role of Particles in Stabilising Foams and Emulsions. *Adv. Colloid Interface Sci.* **2008**, *137*, 57–81.

(4) Gaaseidnes, K.; Turbeville, J. Separation of Oil and Water in Oil Spill Recovery Operations. *Pure Appl. Chem.* **1999**, *71*, 95–101.

(5) Hannisdal, A.; Ese, M.-H.; Hemmingsen, P. V.; Sjöblom, J. Particle-Stabilized Emulsions: Effect of Heavy Crude Oil Components Pre-Adsorbed onto Stabilizing Solids. *Colloids Surf., A* **2006**, *276*, 45–58.

(6) Al-Sahhaf, T.; Elsharkawy, a.; Fahim, M. Stability of Water-in-Crude Oil Emulsions: Effect of Oil Aromaticity, Resins to Asphaltene Ratio, and pH of Water. *Pet. Sci. Technol.* **2008**, *26*, 2009–2022.

(7) Kralova, I.; Sjöblom, J.; Øye, G.; Simon, S.; Grimes, B. a; Paso, K. Heavy Crude Oils/particle Stabilized Emulsions. *Adv. Colloid Interface Sci.* **2011**, *169*, 106–127.

(8) Drexler, S.; Faria, J.; Ruiz, M. P.; Harwell, J. H.; Resasco, D. E. Amphiphilic Nanohybrid Catalysts for Reactions at the Water/Oil Interface in Subsurface Reservoirs. *Energy Fuels* **2012**, *26*, 2231−2241.
(9) Aveyard, R.; Binks, B. P.; Clint, J. H. Emulsions Stabilised Solely by Colloidal Particles. *Adv. Colloid Interface Sci.* **2003**, *100−102*, 503−546.
(10) Zeng, C.; Bissig, H.; Dinsmore, a. D. Particles on Droplets: From Fundamental Physics to Novel Materials. *Solid State Commun.* **2006**, *139*, 547−556.
(11) Dickinson, E. Food Emulsions and Foams: Stabilization by Particles. *Curr. Opin. Colloid Interface Sci.* **2010**, *15*, 40−49.
(12) Binks, B. P. Particles as Surfactants—Similarities and Differences. *Curr. Opin. Colloid Interface Sci.* **2002**, *7*, 21−41.
(13) Binks, B. P.; Fletcher, P. D. I. Particles Adsorbed at the Oil−Water Interface: A Theroretical Comparision between Spheres of Uniform Wettability and "Janus" Particles. *Langmuir* **2001**, *17*, 4708−4710.
(14) Adams, D. J.; Adams, S.; Melrose, J.; Weaver, A. C. Influence of Particle Surface Roughness on the Behaviour of Janus Particles at Interfaces. *Colloids Surf., A* **2008**, *317*, 360−365.
(15) Tanaka, T.; Okayama, M.; Minami, H.; Okubo, M. Dual Stimuli-Responsive "Mushroom-like" Janus Polymer Particles as Surfactants Particulate. *Langmuir* **2010**, *26*, 11732−11736.
(16) Jiang, S.; Chen, Q.; Tripathy, M.; Luijten, E.; Schweizer, K. S.; Granick, S. Janus Particle Synthesis and Assembly. *Adv. Mater.* **2010**, *22*, 1060−1071.
(17) Tu, F.; Lee, D. Shape-Changing and Amphiphilicity-Reversing Janus Particles with pH-Responsive Surfactant Properties. *J. Am. Chem. Soc.* **2014**, *136*, 9999−10006.
(18) Hong, L.; Cacciuto, A.; Luijten, E.; Granick, S. Clusters of Charged Janus Spheres. *Nano Lett.* **2006**, *6*, 2510−2514.
(19) Hong, L.; Cacciuto, A.; Luijten, E.; Granick, S. Clusters of Amphiphilic Colloidal Spheres. *Langmuir* **2008**, *24*, 621−625.
(20) Qiang, W.; Wang, Y.; He, P.; Xu, H.; Gu, H.; Shi, D. Synthesis of Asymmetric Inorganic/Polymer Nanocomposite Particles via Localized Substrate Surface Modification and Miniemulsion Polymerization. *Langmuir* **2008**, *24*, 606−608.
(21) Israelachvili, J. N. *Intermolecular and Surface Forces*, 3rd ed.; Academic Press: Burlington, MA, 2010.
(22) Park, B. J.; Brugarolas, T.; Lee, D. Janus Particles at an Oil−Water Interface. *Soft Matter* **2011**, *7*, 6413−6417.
(23) Park, B. J.; Lee, D. Equilibrium Orientation of Nonspherical Janus Particles at Fluid−Fluid Interfaces. *ACS Nano* **2012**, *6*, 782−790.
(24) Isa, L.; Samudrala, N.; Dufresne, E. R. Adsorption of Sub-Micron Amphiphilic Dumbbells to Fluid Interfaces. *Langmuir* **2014**, *30*, 5057−5063.
(25) De Folter, J. W. J.; Hutter, E. M.; Castillo, S. I. R.; Klop, K. E.; Philipse, A. P.; Kegel, W. K. Particle Shape Anisotropy in Pickering Emulsions: Cubes and Peanuts. *Langmuir* **2014**, *30*, 955−964.
(26) Yang, J.; Sargent, E. H.; Kelley, S. O.; Ying, J. Y. A General Phase-Transfer Protocol for Metal Ions and Its Application in Nanocrystal Synthesis. *Nat. Mater.* **2009**, *8*, 683−689.
(27) Li, D.; Zhao, B. Temperature-Induced Transport of Thermosensitive Hairy Hybrid Nanoparticles between Aqueous and Organic Phases. *Langmuir* **2007**, *23*, 2208−2217.
(28) Wu, Y.; Zhang, C.; Qu, X.; Liu, Z.; Yang, Z. Light-Triggered Reversible Phase Transfer of Composite Colloids. *Langmuir* **2010**, *26*, 9442−9448.
(29) Stocco, A.; Chanana, M.; Su, G.; Cernoch, P.; Binks, B. P.; Wang, D. Bidirectional Nanoparticle Crossing of Oil−Water Interfaces Induced by Different Stimuli: Insight into Phase Transfer. *Angew. Chem., Int. Ed.* **2012**, *51*, 9647−9651.
(30) Karanikas, J. M. Unconventional Resources: Cracking the Hydrocarbon Molecules In Situ. *J. Pet. Technol.* **2012**, 68−75.
(31) Judzis, A.; Felder, R.; Curry, D.; Seiller, B.; Pope, G. A.; Burnett, D.; Torp, T. A.; Neal, J.; Krohn, C.; Karanikas, J. M.; et al. The Five R & D Grand Challenges Plus One. *J. Pet. Technol.* **2011**, 34−35.
(32) Liu, S.; Bai, S. Q.; Zheng, Y.; Shah, K. W.; Han, M. Y. Composite Metal−Oxide Nanocatalysts. *ChemCatChem.* **2012**, *4*, 1462−1484.
(33) Wang, S.; Ma, F.; Zhao, H.; Wu, N. Bulk Synthesis of Metal−Organic Hybrid Dimers and Their Propulsion under Electric Fields. *ACS Appl. Mater. Interfaces* **2014**, *6*, 4560−4569.
(34) Zhang, F.; Cao, L.; Yang, W. Preparation of Monodisperse and Anion-Charged Polystyrene Microspheres Stabilized with Polymerizable Sodium Styrene Sulfonate by Dispersion Polymerization. *Macromol. Chem. Phys.* **2010**, *211*, 744−751.
(35) Sheu, H. R.; El-Aasser, M. S.; Vanderhoff, J. W. Phase Separation in Polystyrene Latex Interpenetrating Polymer Networks. *J. Polym. Sci., Part A: Polym. Chem.* **1990**, *28*, 629−651.
(36) Kim, J.-W.; Larsen, R. J.; Weitz, D. A. Synthesis of Nonspherical Colloidal Particles with Anisotropic Properties. *J. Am. Chem. Soc.* **2006**, *128*, 14374−14377.
(37) Mock, E. B.; De Bruyn, H.; Hawkett, B. S.; Gilbert, R. G.; Zukoski, C. F. Synthesis of Anisotropic Nanoparticles by Seeded Emulsion Polymerization. *Langmuir* **2006**, *22*, 4037−4043.
(38) Kim, J.-W.; Lee, D.; Shum, H. C.; Weitz, D. A. Colloid Surfactants for Emulsion Stabilization. *Adv. Mater.* **2008**, *20*, 3239−3243.
(39) Park, J.-G.; Forster, J. D.; Dufresne, E. R. High-Yield Synthesis of Monodisperse Dumbbell-Shaped Polymer Nanoparticles. *J. Am. Chem. Soc.* **2010**, *132*, 5960−5961.
(40) Sherrington, D. C. Preparation, Structure and Morphology of Polymer Supports. *Chem. Commun.* **1998**, 2275−2286.
(41) Kim, J. W.; Larsen, R. J.; Weitz, D. a. Uniform Nonspherical Colloidal Particles with Tunable Shapes. *Adv. Mater.* **2007**, *19*, 2005.
(42) Sheu, H. R.; El-Aasser, M. S.; Vanderhoff, J. W. Uniform Nonspherical Latex Particles as Model Interpenetrating Polymer Networks. *J. Polym. Sci., Part A: Polym. Chem.* **1990**, *28*, 653−667.
(43) Qiang, W.; Wang, Y.; He, P.; Xu, H.; Gu, H.; Shi, D. Synthesis of Asymmetric Inorganic/Polymer Nanocomposite Particles via Localized Substrate Surface Modification and Miniemulsion Polymerization. *Langmuir* **2008**, *24*, 606−608.
(44) Wang, Y.; Zhang, C.; Tang, C.; Li, J.; Shen, K.; Liu, J.; Qu, X.; Li, J.; Wang, Q.; Yang, Z. Emulsion Interfacial Synthesis of Asymmetric Janus Particles. *Macromolecules* **2011**, *44*, 3787−3794.
(45) Speight, J. G. *The Chemistry and Technology of Petroleum*; 5th ed.; CRC Press: Boca Raton, FL, 2014.
(46) Hyne, N. *Nontechnical Guide to Petroleum Geology, Exploration, Drilling, and Production*, 2nd ed.; PennWell Books: Tulsa, OK, 2001.
(47) Plueddemann, E. P. *Silane Coupling Agents*, 2nd ed.; Springer: New York, 1991.